American Mineralogist, Volume 98, pages 141–153, 2013

A thermodynamic model for silica and aluminum in alkaline solutions with high ionic strength at elevated temperatures up to 100 °C: Applications to zeolites

YONGLIANG XIONG*

Sandia National Laboratories, Carlsbad Programs Group, 4100 National Parks Highway, Carlsbad, New Mexico 88220, U.S.A.

ABSTRACT

In this study, a thermodynamic model for silica and aluminum in high ionic strength solutions at elevated temperatures up to 100 °C is constructed. Pitzer equations are utilized for the thermodynamic model construction. This model is valid up to ionic strengths of ~24 molal (m) in NaOH solutions with silicate concentrations up to ~1.5 m. The speciation of silica (including monomers and polymers) and aluminum at elevated temperatures is taken into account. Also, the equilibrium constants for silicic acid and its polymer species (H_4SiO_4, $H_5Si_2O_7^-$, $H_4Si_2O_7^{2-}$, and $H_5Si_3O_7^{3-}$) at elevated temperatures up to 100 °C, are obtained based on theoretical calculations. Using this thermodynamic model, thermodynamic properties, including equilibrium constants, and respective reaction enthalpies are obtained for sodium silicates, zeolite A, and the amorphous form of zeolite A, based on solubility experiments at elevated temperatures. The equilibrium constants for zeolite A and amorphous precursor of zeolite A regarding the following reactions up to 100 °C,

$$NaAlSiO_4{\cdot}2.25H_2O(cr) + 4H^+ = Na^+ + Al^{3+} + H_4SiO_4(aq) + 2.25H_2O(l) \quad (1)$$

and

$$NaAlSiO_4{\cdot}2.25H_2O(am) + 4H^+ = Na^+ + Al^{3+} + H_4SiO_4(aq) + 2.25H_2O(l) \quad (2)$$

can be expressed as follows

$$\log K_1 = \frac{7963 \pm 327}{T} - 16.46 \pm 0.96 \quad (3)$$

and

$$\log K_2 = \frac{12971 \pm 160}{T} - 30.80 \pm 0.50 \quad (4)$$

where T is temperature in Kelvin.

The enthalpy of formation from elements, Gibbs free energy of formation from elements, and standard entropy derived for zeolite A and the amorphous form of zeolite A with the chemical formulas mentioned above at 25 °C and 1 bar are –2738 ± 5 kJ/mol, –2541 ± 2 kJ/mol, 373 ± 10 J/(K·mol); and –2642 ± 3 kJ/mol, –2527 ± 2 kJ/mol, and 648 ± 10 J/(K·mol), respectively. The enthalpy of formation from elements for zeolite A derived in this study based on solubility experiments in hydrothermal solutions agrees well with those obtained by calorimetric measurements and by theoretical calculations.

Keywords: Pitzer equation, solution chemistry, sodium silicates, hydrothermal synthesis

INTRODUCTION

Zeolites have numerous applications ranging from their usage as absorbents and catalysts to wasteforms for radioactive iodine (^{129}I) and for contaminated electrolytes from electrorefinery of used nuclear fuel (e.g., Sheppard et al. 2006). The formation of zeolites occurs under alkaline conditions in solutions typically with high ionic strengths. For instance, in the hydrothermal synthesis of zeolite A, zeolite X, and mordenite, NaOH solutions ranging from 0.6 to 2 molal (m) were frequently used (e.g., Čižmek et al. 1991a, 1991b, 1992; Šefčik and McCormick 1997a). It has also been noted that in high-level nuclear waste processing, concentrated waste liquor is produced by evaporation at elevated temperatures up to 140 °C, and the resulting concentrated waste liquor can have NaOH concentrations up to ~7 m (Addai-Mensah et al. 2004). In laboratory experiments designed to simulate the concentrated waste liquor from high-level nuclear waste processing, the precipitation of zeolite A and the amorphous form zeolite A from the simulated concentrated waste liquor has been observed (Addai-Mensah et al. 2004). Finally, at the Hanford site in Washington State, the leakage of

* E-mail: yxiong@sandia.gov

0003-004X/13/0001–141$05.00/DOI: http://dx.doi.org/10.2138/am.2013.4089

the alkaline solutions with high ionic strengths contained in the waste tanks into sediments resulted in formation of cancrinite and sodalite, which belong to the zeolite family, in the sediment below a waste tank (Chorover et al. 2003; Mashal et al. 2004; Serne et al. 2002; Zhao et al. 2004).

While there are experimental data on zeolites (see Table 1), the formation of zeolites at elevated temperatures is not well understood owing to the lack of reliable thermodynamic model(s). Furthermore, there is the current inability to address simultaneously the behavior of both silica and aluminum, the two most rock-forming elements, in high ionic strength solutions at elevated temperatures. The high ionic strength nature of solutions and high concentrations of silica are the factors contributing to the difficulties associated with the development of a thermodynamic model at elevated temperatures for zeolites. For instance, when zeolite A is formed, the concentration of silica can reach up to 0.12 m (Šefčik and McCormick 1997b). The nature of high ionic strength solutions requires that the activity coefficient model be valid to high ionic strengths. The high concentrations of silica require that polymers of silica species be considered, as polymerized silica species might become important when silica concentrations are higher than 0.01 m (e.g., Felmy et al. 2001).

A thermodynamic model applicable to concentrated solutions at elevated temperatures is therefore needed to predict the formation of zeolites including zeolite A, amorphous precursor of zeolite A, cancrinite, and sodalite, at elevated temperatures. In addition, such a model would provide valuable guidance in the synthesis of zeolites. A thermodynamic model would also provide

TABLE 1. Sources and experimental conditions for solubility experiments on sodium silicates, zeolite A and amorphous precursor of zeolite A from which solubility data are used for computation of equilibrium constants

Solubility-controlling phase	Authors	T °C	Aqueous solution, NaOH, Molal, m	ΣSi, Molal, m	ΣAl, Molal, m	Remarks
$3Na_2O•2SiO_2•11H_2O$	Sprauer and Pearce (1940)	25	12.3–18.8	7.93×10^{-2} to 3.62×10^{-1}	None	Approaching equilibrium: from supersaturation. Experimental duration: one month. Usage of data: calculation of Pitzer parameter.
$Na_3HSiO_4•5H_2O$	Baker et al. (1950)	50	12.6–19.6	2.78×10^{-1} to 1.47	None	Approaching equilibrium: from both undersaturation and supersaturation. Experimental duration: a few weeks. Usage of data: calculation of Pitzer parameter.
$Na_3HSiO_4•2H_2O$	Baker et al. (1950)	50, 70, 90	15.9–23.2	7.43×10^{-2} to 2.14	None	Approaching equilibrium: from both undersaturation and supersaturation. Experimental duration: a few weeks. Usage of data: calculation of Pitzer parameter.
Zeolite A	Ciric (1968)	100	0.459–1.72	6.26×10^{-3} to 2.76×10^{-2}	1.31×10^{-1} to 1.78×10^{-1}	Approaching equilibrium: from supersaturation. Experimental duration: longer than 100 min. Usage of data: calculation of log K for zeolite A.
	Zhdanov (1971)	90	1.63–4.27	2.11×10^{-3} to 2.69×10^{-2}	2.69×10^{-2} to 1.29	Approaching equilibrium: from undersaturation. Experimental duration: longer than 100 min. Usage of data: calculation of log K for zeolite A.
	Wieker and Fahlke (1985)	80	2.17	2.37×10^{-2}	1.96×10^{-2}	Approaching equilibrium: from undersaturation. Experimental duration longer: than 100 min. Usage of data: calculation of log K for zeolite A.
	Čižmek et al. (1991a)	65, 70, 80	1.02–2.06	1.17×10^{-2} to 1.83×10^{-2}	1.11×10^{-2} to 1.83×10^{-2}	Approaching equilibrium: from undersaturation. Experimental duration longer than 100 min. Usage of data: calculation of log K for zeolite A.
	Myatt (1994)	90	2.49–3.34	8.47×10^{-3} to 6.13×10^{-2}	1.04×10^{-2} to 1.25×10^{-1}	Approaching equilibrium from supersaturation. Experimental duration: longer than 100 min. Usage of data: calculation of log K for zeolite A.
	Ejaz and Graham (1999)	30, 50, 65, 80	3.04–4.46	3.28×10^{-3} to 1.69×10^{-2}	4.32×10^{-3} to 1.55×10^{-2}	Approaching equilibrium: from undersaturation. Experimental duration: longer than 100 min. Usage of data: calculation of log K for zeolite A.
	Kosanović et al. (2000)	70	2.05	1.51×10^{-2} to 1.81×10^{-2}	1.46×10^{-2} to 1.71×10^{-2}	Approaching equilibrium: from undersaturation. Experimental duration: longer than 100 min. Usage of data: calculation of log K for zeolite A.
	Addai-Mensal et al. (2004)	30, 65	3.02–6.31	1.19×10^{-2} to 4.63×10^{-2}	1.42×10^{-2} to 5.43×10^{-2}	Approaching equilibrium: from both undersaturation and supersaturation. Experimental duration: longer than 50 min. Usage of data: calculation of log K for zeolite A.
	Bosnar et al. (2005)	80	1.49–1.58	8.63×10^{-3} to 6.15×10^{-2}	2.06×10^{-3} to 1.03×10^{-2}	Approaching equilibrium: from supersaturation. Experimental duration longer than 100 min. Usage of data: calculation of log K for zeolite A.
Amorphous precursor of zeolite A	Ejaz and Graham (1999)	30, 50, 65, 80	3.04–4.46	4.70×10^{-2} to 7.57×10^{-2}	3.48×10^{-2} to 5.54×10^{-2}	Approaching equilibrium: from undersaturation. Experimental duration: longer than 100 min. Usage of data: calculation of log K for amorphous zeolite A.
	Addai-Mensal et al. (2004)	30, 65	3.02–6.31	7.09×10^{-2} to 2.20×10^{-1}	7.99×10^{-2} to 2.19×10^{-1}	Approaching equilibrium: from both undersaturation and supersaturation. Experimental duration: longer than 50 min. Usage of data: calculation of log K for amorphous zeolite A.

a better understanding of interactions of waste solutions with the sediments, like the interactions observed in the Hanford studies mentioned above. Consequently, the objective of this study is to develop a thermodynamic model for aluminum and silica species at elevated temperatures valid to high ionic strengths. Using this model, equilibrium constants for sodium silicates, zeolite A, and amorphous precursor of zeolite A can be retrieved from hydrothermal experiments. Applications of the model to other zeolite species will be presented in the future.

THE THERMODYNAMIC MODEL

In this study, the standard state for a solid phase is defined as its pure end-member with unit activity at temperatures and pressures of interest. The standard state of the solvent in aqueous solutions is pure solvent at temperatures and pressures of interest. The standard state for an aqueous solute is a hypothetical 1 molal (m) solution referred to infinite dilution at temperatures and pressures of interest. Gibbs free energies and enthalpies of formation reported in this study correspond to the formation from chemical elements at their reference states.

The Pitzer model is adopted in this study for calculations of activity coefficients of aqueous species. The detailed descriptions about Pitzer equations are provided in Pitzer (1991). In the following, an equation for calculation of the activity coefficient of $Al(OH)_4^-$ in NaOH medium without consideration of triple interactions in the Pitzer model is provided as an example,

$$\ln\gamma = -A_\phi\left[\frac{\sqrt{I_m}}{1+1.2\sqrt{I_m}}+\frac{2}{1.2}\ln(1+1.2\sqrt{I_m})\right]+ m\left\{2\beta^{(0)}+\frac{2\beta^{(1)}}{\alpha^2\times I_m}\left[1-(1+\alpha\sqrt{I_m}-\frac{\alpha^2 I_m}{2})e^{-\alpha\sqrt{I_m}}\right]\right\}+\frac{3m^2}{2}C^\phi \quad (1)$$

where γ is activity coefficient; A_ϕ is Deby-Hückel slope for osmotic coefficient; I_m is ionic strength on molality scale; m is molality of Na^+; α is equal to 2; and $\beta^{(0)}$, $\beta^{(1)}$, and C^ϕ are Pitzer binary interaction coefficients between Na^+ and $Al(OH)_4^-$.

The uncertainties reported in this study are two standard deviations (2σ). Error propagations are calculated based on uncertainties associated with regressions and equilibrium constants in the model. In some cases, especially for $\Delta_f G$, $\Delta_f H$, and $S°$, uncertainties could be underestimated, as uncertainties for auxiliary data are not available, and therefore not included.

Thermodynamic constants and Pitzer interaction parameters of Si and Al aqueous species chosen and extrapolated from the literature

The following monomer, dimer, and trimer silica species are considered in this thermodynamic model:

$$H_4SiO_4 = H^+ + H_3SiO_4^- \quad (2)$$
$$H_3SiO_4^- = H^+ + H_2SiO_4^{2-} \quad (3)$$
$$2H_4SiO_4 = H^+ + H_5Si_2O_7^- + H_2O \quad (4)$$
$$H_5Si_2O_7^- = H^+ + H_4Si_2O_7^{2-} \quad (5)$$
$$3H_4SiO_4 = 3H^+ + H_5Si_3O_{10}^{3-} + 2H_2O. \quad (6)$$

The equilibrium constants for reaction 2 are obtained from Fleming and Crerar (1982) (Table 2). The first dissociation constants of monomeric silicic acid from Fleming and Crerar (1982) are selected, as these authors regressed several experimentally determined first dissociation constants for monomeric silicic acid from previous studies, including the most reliable values determined via the solubility and potentiometric methods (e.g., Seward 1974; Busey and Mesmer 1977). However, uncertainties associated with their dissociation constants were not given in Fleming and Crerar (1982). In this study, uncertainties are assigned based on the respective benchmark values of Busey and Mesmer (1977). The second dissociation constants ($\log K_2$) of monomeric silicic acid at elevated temperatures (reaction 3) are estimated by using the one-term isocoulombic approach with phosphoric acid as the model substance as employed before (e.g., Xiong 2003, 2007) (Table 2), based on the $\log K_2$ at 25 °C from Hershey and Millero (1986). The equilibrium constants at 25 °C for dimer and trimer silica species (reactions 4–6) are from Felmy et al. (2001). The $\log K$ at elevated temperatures for those dimer and trimer silica species are also predicted in this study in a manner similar to that described above for the $\log K_2$ of monomer silicic acid. They are tabulated in Table 2. The uncertainty for $\log K$ values of well balanced isocoulombic reactions is usually within ±0.50 up to 200 °C (Gu et al. 1994). Therefore, an uncertainty of ±0.25 is assigned to all predicted values at elevated temperatures up to 100 °C.

An example of a well-balanced isocoulombic reaction is given in the following,

$$H_4SiO_4 + H_2PO_4^- = H_3PO_4 + H_3SiO_4^-. \quad (7)$$

In the above reaction, H_4SiO_4 with zero charge on the left side is balanced by H_3PO_4 with zero charge on the right side. Similarly, $H_2PO_4^-$ with one negative charge on the left side is balanced by $H_3SiO_4^-$ with one negative charge on the right side.

It should be noted that regarding polymers of silica species, only dimer and trimer are considered in this study, and tetramer and hexamer are excluded. This consideration is primarily based on numerous studies that have indicated that monomer, dimer, and trimer are adequate in descriptions of silica solutions with high concentrations (e.g., Čižmek et al. 1992; Sefćik and McCormick 1997b; Hunt et al. 2011). For instance, in a Raman spectroscopic study on silica speciation in concentrated silica solutions up to 5.0 m with KOH as a supporting solution ranging from 0.08 to 8.0 m conducted by Hunt et al. (2011), the authors demonstrate that monomer, dimer, and trimer species are sufficient to describe the silica species in highly concentrated silicate solutions with total silica concentrations up to 5.0 m.

The following species are incorporated into the aluminum thermodynamic model:

$$Al(OH)_4^- = Al^{3+} + 4OH^-. \quad (8)$$

Equilibrium constants for reaction 8 at various temperatures are tabulated in Table 3.

The equilibrium constants for reaction 8 are obtained from Wesolowski (1992) based on the following reaction:

TABLE 2. Equilibrium constants for silica and aluminum species considered in this study up to 100 °C

Reaction	*T*, °C	log *K*	Reference
$H_4SiO_4 = H^+ + H_3SiO_4^-$	25	−9.68 ± 0.14*	Fleming and Crerar (1982)
	50	−9.34 ± 0.16*	Fleming and Crerar (1982)
	75	−9.10 ± 0.17*	Fleming and Crerar (1982)
	100	−8.94 ± 0.16*	Fleming and Crerar (1982)
$H_3SiO_4^- = H^+ + H_2SiO_4^{2-}$	25	−13.45 ± 0.07	Hershey and Millero (1986)
	50	−12.95 ± 0.25†	This study
	75	−12.56 ± 0.25†	This study
	100	−12.28 ± 0.25†	This study
$2H_4SiO_4 = H^+ + H_5Si_2O_7^- + H_2O$	25	−8.50‡	Felmy et al. (2001)
	50	−8.14 ± 0.25†	This study
	75	−7.86 ± 0.25†	This study
	100	−7.65 ± 0.25†	This study
$H_5Si_2O_7^- = H^+ + H_4Si_2O_7^{2-}$	25	−10.90‡	Felmy et al. (2001)
	50	−10.59 ± 0.25†	This study
	75	−10.38 ± 0.25†	This study
	100	−10.24 ± 0.25†	This study
$3H_4SiO_4 = 3H^+ + H_5Si_3O_{10}^{3-} + 2H_2O$	25	−29.40‡	Felmy et al. (2001)
	50	−28.75 ± 0.25†	This study
	75	−28.34 ± 0.25†	This study
	100	−28.11 ± 0.25†	This study
$Al(OH)_4^- = Al^{3+} + 4OH^-$	25	−34.05 ± 0.05	Derived from Wesolowski (1992)
	50	−33.44 ± 0.05	Derived from Wesolowski (1992)
	75	−33.11 ± 0.05	Derived from Wesolowski (1992)
	100	−32.99 ± 0.05	Derived from Wesolowski (1992)
$Al(OH)_4^- + H_2SiO_4^{2-} = Al(OH)_3HSiO_4^{3-} + H_2O(l)$	20	−0.42 ± 0.10	This study§, estimated from log β_1' (Gout et al. 2000) with the SIT model
	25	−0.42 ± 0.15	This study§
	50	−0.38 ± 0.25†	This study§
	75	−0.35 ± 0.25†	This study§
	100	−0.33 ± 0.25†	This study§

* Uncertainties were not given in Fleming and Crerar (1982). Uncertainties are assigned based on the respective benchmark values of Busey and Mesmer (1977).
† An uncertainty of ±0.25 is assigned to all predicted values at elevated temperatures up to 100 °C. See text for details.
‡ Uncertainties were not given in Felmy et al. (2001).
§ The complex, $Al(OH)_3HSiO_4^{3-}$, is used to test whether it can improve the modeling at 30 and 50 °C only.

$$Al(OH)_4^- = Al(OH)_3(cr, gibbsite) + OH^- \quad (9)$$

in combination with the equilibrium constants for the following reaction calculated from SUPCRT (Johnson et al. 1992):

$$Al(OH)_3(cr, gibbsite) = Al^{3+} + 3OH^-. \quad (10)$$

In this study, the hydrolysis constants of $Al(OH)_4^-$ described above determined by Wesolowski (1992) are selected because they are consistent with the respective Pitzer parameters adopted in this study. Although Tagirov and Schott (2001) provided the revised hydrolysis constants for $Al(OH)_4^-$, those values are not adopted in this study, as the activity coefficient model employed by Tagirov and Schott (2001) is different from the Pitzer model.

In the present model, regarding aluminum species in alkaline solutions, only $Al(OH)_4^-$ is included, and no aluminum polymeric species are considered. This consideration is based on the fact that aqueous aluminum species exists as $Al(OH)_4^-$ in neutral and basic solutions when $m_{\Sigma Al}$ is less than 1.5 m (Moolenaar et al. 1970; Baes and Mesmer 1976; Castet et al. 1993). The formation of aluminum polymeric species requires $m_{\Sigma Al} \geq 1.5$ m (Moolenaar et al. 1970). In the presence of silica, aluminum concentrations are much lower than 1.5 m. As solutions in which zeolites are formed contain both silica and aluminum, aluminum polymeric species will not be important.

It should be noted that although Zhou et al. (2003) also determined the Pitzer interaction parameters for the interaction between Na^+ and $Al(OH)_4^-$, the Pitzer parameters of Wesolowski (1992) are adopted in the current model as they are consistent with the hydrolysis constants of $Al(OH)_4^-$ used in this study.

In addition, there are some studies suggesting that the aqueous Al-Si complex(es) such as $Al(OH)_3H_3SiO_4^-$ and $SiAlO_3(OH)_4^{3-}$ might be present in aqueous solutions (e.g., Pokrovski et al. 1998; Salvi et al. 1998; Gout et al. 2000). Salvi et al. (1998) suggested that $Al(OH)_3H_3SiO_4^-$ with log $\beta_1 = 2.32$ could be present at 300 °C, corresponding to the following reaction,

$$Al(OH)_4^- + H_4SiO_4(aq) = Al(OH)_3H_3SiO_4^- + H_2O(l). \quad (11)$$

Gout et al. (2000) mentioned that a weak complex, $SiAlO_3(OH)_4^{3-}$ [also formulated as $Al(OH)_3HSiO_4^{3-}$] with log $\beta_1' = 0.53$ ($I = 1.2$ m), could be present at 20 °C, with reference to the following reaction,

$$Al(OH)_4^- + H_2SiO_4^{2-} = Al(OH)_3HSiO_4^{3-} + H_2O(l). \quad (12)$$

The β_1 at infinite dilution can be expressed as

$$\begin{aligned}\beta_1 &= \frac{(m_{Al(OH)_3HSiO_4^{3-}})(\gamma_{Al(OH)_3HSiO_4^{3-}})(a_{H_2O})}{(m_{Al(OH)_4^-})(\gamma_{Al(OH)_4^-})(m_{H_2SiO_4^{2-}})(\gamma_{H_2SiO_4^{2-}})} \\ &= \frac{(m_{Al(OH)_3HSiO_4^{3-}})}{(m_{Al(OH)_4^-})(m_{H_2SiO_4^{2-}})} \times \frac{(\gamma_{Al(OH)_3HSiO_4^{3-}})(a_{H_2O})}{(\gamma_{Al(OH)_4^-})(\gamma_{H_2SiO_4^{2-}})} \\ &= \beta_1^I \times \frac{(\gamma_{Al(OH)_3HSiO_4^{3-}})(a_{H_2O})}{(\gamma_{Al(OH)_4^-})(\gamma_{H_2SiO_4^{2-}})}\end{aligned} \quad (13)$$

Other studies (e.g., Yokoyama et al. 1988) suggested that the formation of aqueous complex(es) of aluminum with silica is likely in dilute NaOH solutions at room temperature, but such a complex is absent in high alkaline solutions such as 1.0

TABLE 3. Pitzer interaction parameters employed in this study

Binary interaction parameters				
Interaction pair	$\beta^{(0)}$	$\beta^{(1)}$	C^{φ}	References
Na^+-$H_3SiO_4^-$	0.043 ± 0.019	0.24 ± 0.11		Hershey and Millero (1986)
Na^+-$H_2SiO_4^{2-}$	0.32 ± 0.08	0.13 ± 0.50		Hershey and Millero (1986)
Na^+-$H_5Si_2O_7^-$	–0.0571 ± 0.04	0.34 ± 0.13		This Study*
Na^+-$H_4Si_2O_7^{2-}$	–0.0227 ± 0.06	1.56 ± 0.40		This Study†
Na^+-$H_5Si_3O_{10}^{3-}$	0.078 ± 0.03	4.29 ± 0.80		This Study‡
Na^+-$Al(OH)_3HSiO_4^{3-}$	0.078 ± 0.03	4.29 ± 0.80		This Study §
Na^+-$Al(OH)_4^-$	0.051	0.25	–0.00090	Wesolowski (1992)¶
Interaction involving neutral species and mixing parameters				
Interaction pair	λ_{ij}	θ_{ij}	Ψ_{ijk}	References
Na^+-$H_4SiO_4^0$	0.0925			Azaroual et al. (1997)¶
OH^--$H_2SiO_4^{2-}$		–0.0812 ± 0.003, $(\partial\theta_{ij})/(\partial T)_P = -9.35 \pm 0.44 \times 10^{-5}$		This Study‖
OH^--$H_2SiO_4^{2-}$-Na^+			–0.017 ± 0.02	This Study‖

* Calculated from the estimation method of Plyasunov et al. (1998) for 1:1 interaction, based on $\varepsilon[Na^+, Si_2O_2(OH)_5^-]$ of –0.08 ± 0.04, which is from Grenthe et al. (1992). In the method of Plyasunov et al. (1998), uncertainty was not given to $\beta^{(1)}$. The uncertainty assigned here is two standard deviations from the average $\beta^{(1)}$ for 1:1 interaction computed in Plyasumov et al. (1998).

† Calculated from the estimation method of Plyasunov et al. (1998) for 1:2 interaction, based on $\varepsilon[Na^+, Si_2O_3(OH)_4^{2-}]$ of –0.15 ± 0.06 from Grenthe et al. (1992). In the method of Plyasunov et al. (1998), uncertainty was not given to $\beta^{(1)}$. The uncertainty assigned here is two standard deviations from the average $\beta^{(1)}$ for 1:2 interaction computed in Plyasumov et al. (1998).

‡ Calculated from the estimation method of Plyasunov et al. (1998) for 1:3 interaction, based on $\varepsilon[Na^+, Si_3O_6(OH)_3^{3-}]$ of –0.25 ± 0.03 from Grenthe et al. (1992). In the method of Plyasunov et al. (1998), uncertainty was not given to $\beta^{(1)}$. The uncertainty assigned here is two standard deviations from the average $\beta^{(1)}$ for 1:3 interaction computed in Plyasumov et al. (1998).

§ Interaction parameters are assigned to be the same as those for Na^+-$H_5Si_3O_{10}^{3-}$.

¶ Uncertainties were not given in Wesolowski (1992) and Azaroual et al. (1997), respectively.

‖ Evaluated from solubility data of $3Na_2O{\cdot}2SiO_2{\cdot}11H_2O$ in NaOH solutions up to ~19 m from Sprauer and Pearce (1940). The temperature dependence of θ_{ij}, $(\partial\theta_{ij})/(\partial T)_P$, is evaluated from solubility data of $Na_3HSiO_4{\cdot}5H_2O$ at 50 °C, and of $Na_3HSiO_4{\cdot}2H_2O$ at 50, 70, and 90 °C in NaOH solutions up to ~24 m from Baker et al. (1950).

m NaOH, typical of solutions in which zeolites are stable. Yokoyama et al. (1988) also demonstrated that higher temperatures destabilize the complex of aluminum and silicate that formed in dilute NaOH solutions.

However, since the presence or absence of Al-Si complexes is an important issue, as an independent constrain on the existence of Al-Si complexes in alkaline solutions, the $Al(OH)_3HSiO_4^{3-}$ complex is tested to see whether it can improve the modeling at 30 and 50 °C (see following sections), as this complex was proposed to be present at 20 °C. In doing this, as there is only one apparent formation constant at one ionic strength (i.e., 1.2 m) in NaCl, the log β_1 at infinite dilution at 20 °C is first estimated by using the Brønsted-Guggenheim-Scatchard SIT model (Grenthe et al. 1992). According to the SIT model regarding Equations 12–13, we have,

$$\log\beta_1 = \log\beta_1^I - 4D + \log a_{H_2O} + \Delta\varepsilon(\text{Eq.12}) \times I_m \quad (14)$$

$$\Delta\varepsilon(\text{Eq.12}) = \varepsilon[Na^+, Al(OH)_3HSiO_4^{3-}] - \varepsilon[Na^+, Al(OH)_4^-] - \varepsilon(Na^+, H_2SiO_4^{2-}) \quad (15)$$

where $\log\beta_1^I$ is the formation constant regarding reaction 12 at a certain ionic strength defined in Equation 13; I_m ionic strength on molal scale; ε values are the SIT interaction coefficients; a_{H_2O} is activity of water; and D is the Debye-Hückel term given below,

$$D = \frac{A_\gamma\sqrt{I_m}}{1 + 1.5\sqrt{I_m}} \quad (16)$$

where A_γ the Debye-Hückel slope for activity coefficient. Substituting $\log\beta_1^I$ = 0.53 at 20 °C from Gout et al. (2000), A_γ = 0.5059 at 20 °C from Helgeson and Kirkham (1974), a_{H_2O} = 0.9600 for 1.2 m NaCl calculated using the EQ3/6 code, $\varepsilon[Na^+, Al(OH)_3HSiO_4^{3-}] \approx \varepsilon[Na^+, Si_3O_6(OH)_3^{3-}] \approx$ = –0.25 ± 0.03, $\varepsilon[Na^+, H_2SiO_4^{2-}] = \varepsilon[Na^+, SiO_2(OH)_2^{2-}]$ = –0.10 ± 0.07, and $\varepsilon[Na^+, Al(OH)_4^-] \approx \varepsilon[Na^+, B(OH)_4^-]$ = –0.07 ± 0.05, all from Grenthe et al. (1992), and I_m = 1.2 m into Equations 14–16, log β_1 is estimated as –0.42 ± 0.10 at 20 °C. As reaction 12 is in a semi-isocoulombic form, the log β_1 at 20 °C is directly extrapolated to 25 °C and other temperatures using the one-term isocoulombic principle (Table 2).

Pitzer interaction parameters in the Na-Si-OH systems obtained in this study

In this study, the Pitzer binary interaction parameters for Na^+-$H_5Si_2O_7^-$, Na^+-$H_4Si_2O_7^{2-}$, and Na^+-$H_5Si_3O_{10}^{3-}$ are calculated according to the method of Plyasunov et al. (1998) based on the respective SIT coefficients for these interactions (Table 3).

The high-order Pitzer parameters, θ_{ij} for OH^--$H_2SiO_4^{2-}$ interaction, and Ψ_{ijk} for OH^--$H_2SiO_4^{2-}$-Na^+ interaction, are evaluated from solubility data of the sodium silicate, $3Na_2O{\cdot}2SiO_2{\cdot}11H_2O$, in NaOH solutions up to ~19 m from Sprauer and Pearce (1940). In addition, $(\partial\theta_{ij})/(\partial T)_P$ for OH^--$H_2SiO_4^{2-}$ interaction is evaluated from solubility data of $Na_3HSiO_4{\cdot}5H_2O$ and $Na_3HSiO_4{\cdot}2H_2O$ at elevated temperatures from Baker et al. (1950) (Table 3).

For the testing purpose, the Pitzer binary interaction parameters for Na^+-$Al(OH)_3HSiO_4^{3-}$ are assumed to be the same as those for Na^+-$H_5Si_3O_{10}^{3-}$ (Table 3).

Sprauer and Pearce (1940) experimentally determined solubilities of $3Na_2O{\cdot}2SiO_2{\cdot}11H_2O$ in NaOH solutions at 25 °C. Their experiments approached equilibrium from supersaturation in about one month (Table 1). Their experiments were in NaOH solutions with very high concentrations up to ~19.0 m. The solubility reaction for $3Na_2O{\cdot}2SiO_2{\cdot}11H_2O$ can be expressed as follows, using H_4SiO_4(aq) as a basis species for silica,

$$3Na_2O{\cdot}2SiO_2{\cdot}11H_2O + 6H^+ = 6Na^+ + 2H_4SiO_4(aq) + 10H_2O(l). \quad (17)$$

The log K for reaction 17 is evaluated as 83.83 ± 0.62 at 25 °C (Table 3) along with θ_{ij} for OH^--$H_2SiO_4^{2-}$ interaction, and Ψ_{ijk} for OH^-–$H_2SiO_4^{2-}$-Na^+ interaction (Table 4).

In Figure 1, predicted solubilities of $3Na_2O{\cdot}2SiO_2{\cdot}11H_2O$ at 25 °C are compared with experimental data from Sprauer and Pearce (1940). From the figure, it is clear that the model reproduces experimental data generally within a factor of ~3.

Baker et al. (1950) investigated solubilities of $Na_3HSiO_4{\cdot}2H_2O$ and $Na_3HSiO_4{\cdot}5H_2O$ in NaOH solutions up to ~24 m at elevated temperatures to 90 °C. Their experiments approached equilibrium from both undersaturation and supersaturation in a few of weeks. The dissolution of $Na_3HSiO_4{\cdot}5H_2O$ can be expressed as:

$$Na_3HSiO_4{\cdot}5H_2O + 3H^+ = 3Na^+ + H_4SiO_4(aq) + 5H_2O(l). \quad (18)$$

Based on solubility data from Baker et al. (1950) on $Na_3HSiO_4{\cdot}5H_2O$, the equilibrium constant for $Na_3HSiO_4{\cdot}5H_2O$ at 50 °C is obtained as 41.50 ± 0.35 (Table 4).

Similarly, the dissolution of $Na_3HSiO_4{\cdot}2H_2O$ can be expressed as:

$$Na_3HSiO_4{\cdot}2H_2O + 3H^+ = 3Na^+ + H_4SiO_4(aq) + 2H_2O(l). \quad (19)$$

Based on solubility data from Baker et al. (1950) on $Na_3HSiO_4{\cdot}2H_2O$, the equilibrium constants for $Na_3HSiO_4{\cdot}2H_2O$ at 50, 70, and 90 °C are obtained as 47.03 ± 0.35, 45.69 ± 0.31, and 46.03 ± 0.30, respectively (Table 4). In combination with experimental data for $Na_3HSiO_4{\cdot}5H_2O$ at 50 °C, the temperature dependence of $\theta_{OH,\,H_2SiO_4^{2-}}$, $(\partial\theta_{ij})/(\partial T)_P$, is also evaluated (Table 3).

In Figure 1, predicted solubilities of $Na_3HSiO_4{\cdot}5H_2O$ and $Na_3HSiO_4{\cdot}2H_2O$ at 50 °C are also compared with experimental data from Baker et al. (1950). For $Na_3HSiO_4{\cdot}5H_2O$, the model

TABLE 4. Equilibrium constants of sodium silicates and zeolites retrieved from solubility experiments in this study*

T, °C	log K ± 2σ	Reaction
25	83.83 ± 0.62	$3Na_2O{\cdot}2SiO_2{\cdot}11H_2O + 6H^+ = 6Na^+ + 2H_4SiO_4(aq) + 10H_2O(l)$
50	47.03 ± 0.35	
70	45.69 ± 0.31	$Na_3HSiO_4{\cdot}2H_2O + 3H^+ = 3Na^+ + H_4SiO_4(aq) + 2H_2O(l)$
90	46.03 ± 0.30	
50	41.50 ± 0.35	$Na_3HSiO_4{\cdot}5H_2O + 3H^+ = 3Na^+ + H_4SiO_4(aq) + 5H_2O(l)$
25	10.24 ± 0.31†	
30	10.23 ± 0.31	
50	7.95 ± 0.30	
65	6.70 ± 0.33	$NaAlSiO_4{\cdot}2.25H_2O$(cr, zeolite A) + $4H^+ = Na^+ + Al^{3+} + H_4SiO_4(aq) + 2.25H_2O$
70	6.54 ± 0.30	
80	5.74 ± 0.45	
90	5.54 ± 0.36	
100	5.34 ± 0.30	
25	12.68 ± 0.35‡	
30	11.94 ± 0.20	$NaAlSiO_4{\cdot}2.25H_2O$(am, zeolite A) + $4H^+ = Na^+ + Al^{3+} + H_4SiO_4(aq) + 2.25H_2O$
50	9.30 ± 0.30	
65	7.84 ± 0.35	
80	5.82 ± 0.22	

* Experimental conditions for hydrothermal experiments from which solubility data are used for computation of equilibrium constants are detailed in text and Table 1.
† Extrapolated to the reference temperature, 25 °C, based on the linear relation between log K and reciprocal temperature in Kelvin for zeolite A.
‡ Extrapolated to the reference temperature, 25 °C, based on the linear relation between log K and reciprocal temperature in Kelvin for amorphous precursor of zeolite A.

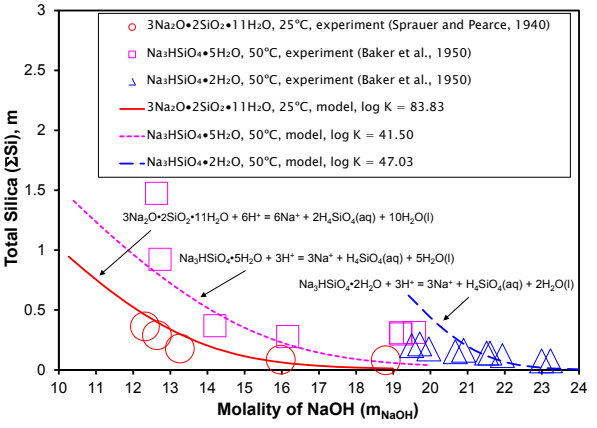

FIGURE 1. Comparison of model predicted solubilities of $3Na_2O{\cdot}2SiO_2{\cdot}11H_2O$ at 25 °C, $Na_3HSiO_4{\cdot}5H_2O$, and $Na_3HSiO_4{\cdot}2H_2O$ at 50 °C, with experimental values. The size of error bars is equal to or smaller than the symbol size. (Color online.)

reasonably reproduces experimental data within a factor of ~1.5, but at $I \approx 19.5$ m, it is within a factor of ~5.5. For $Na_3HSiO_4{\cdot}2H_2O$, the model predicts solubilities at $I \approx 20$ m within a factor of ~3, but it reproduces experimental data at higher ionic strengths within a factor of ~2.

In Figure 2, predicted solubilities of $Na_3HSiO_4{\cdot}2H_2O$ at 70 and 90 °C are compared with experimental data. Figure 2 demonstrates that the model reproduces experimental data within a factor of ~2 for the majority of the data points.

Based on the linear regression of temperature dependence of equilibrium constants, $\Delta_r H$ for reaction 19 is derived as –58 ± 45 (2σ) kJ/mol (Fig. 3, Table 5).

In this study, it is assumed that interaction parameters are constant over the temperature range from 25 to 100 °C, except for θ_{ij} for OH^-–$H_2SiO_4^{2-}$ interaction, which is necessary to modeling solubility of sodium silicates in highly concentrated NaOH solutions. This assumption is based on the observation that the Pitzer interaction parameters do not change significantly over a

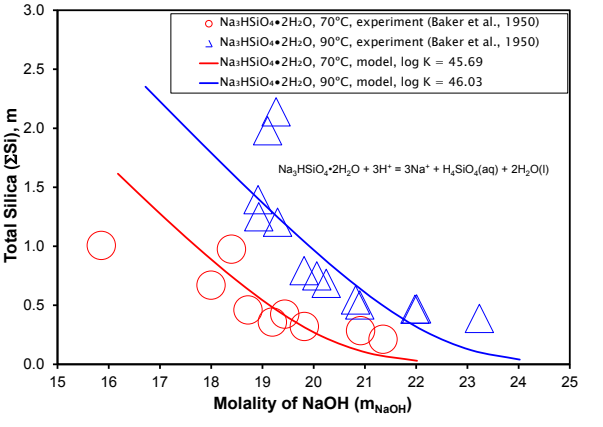

FIGURE 2. Comparison of model predicted solubilities of $Na_3HSiO_4{\cdot}2H_2O$ at 70 and 90 °C with experimental values. The size of error bars is equal to or smaller than the symbol size. (Color online.)

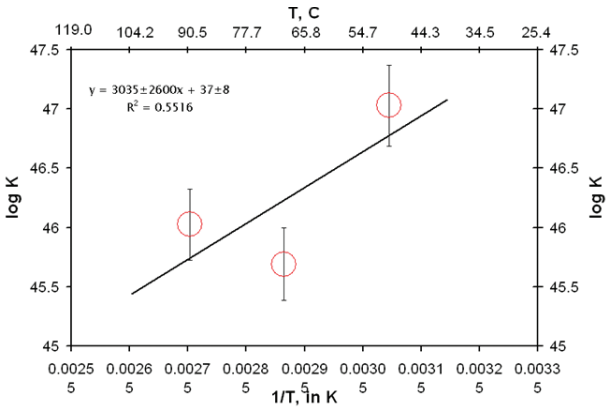

FIGURE 3. A plot showing equilibrium constants of $Na_3HSiO_4 \cdot 2H_2O$ as a function of reciprocal temperatures in Kevin. (Color online.)

narrow range of temperature. For instance, for the interaction of Na^+ with $Al(OH)_4^-$, the temperature derivatives of Pitzer interaction parameters are very small over this temperature range, i.e.,

$$\left(\frac{\partial \beta^{(0)}}{\partial T}\right)_P = 8.0\times10^{-5}, \left(\frac{\partial \beta^{(1)}}{\partial T}\right)_P = 2.7\times10^{-4},$$

and

$$\left(\frac{\partial C^{(\phi)}}{\partial T}\right)_P = 6.9\times10^{-5},$$

based on the respective interaction parameters as a function of temperature from Wesolowski (1992). In addition, in the validation test (see the following section), model-predicted values are in satisfactory agreement with independent experimental values.

The data0.PIT database in the EQ3/6 code can be used to compute activity coefficients by using the Pitzer equations up to 100 °C (Wolery 1992). The original data0.PIT database does not contain the following species: H_4SiO_4(aq), $H_3SiO_4^-$, $H_2SiO_4^{2-}$, $H_5Si_2O_7^-$, $H_4Si_2O_7^{2-}$, $H_5Si_3O_{10}^{3-}$, and $Al(OH)_4^-$. By incorporating the equilibrium constants for the respective reaction detailed in Table 2, and the relevant Pitzer interaction parameters from Hershey and Millero (1986), Wesolowski (1992), Azaroual et al. (1997), and this study tabulated in Table 3 into the data0.PIT database, the PIT database is modified to be able to model high ionic strength solutions with high concentrations of Si and Al up to 100 °C.

Model validation

A validation test is performed for the Na-Si-OH model developed in this study. For this purpose, predicted solubilities of amorphous silica in alkaline solution with a wide range ionic strengths are compared with experimental data, which are independent from the model development. The dissolution of amorphous silica can be expressed as,

$$SiO_2(am) + 2H_2O = 2H^+ + H_2SiO_4^{2-}. \quad (20)$$

The log K for reaction 20, is –25.81 from Weber and Hunt (2003). In Figure 4, predicted solubilities of amorphous silica are compared with experimental data in NaOH solutions at 25 °C from Alexander et al. (1954), and in NaOH + $NaNO_3$ mixtures at 25 °C from Weber and Hunt (2003). From Figure 4, it is obvious that solubilities predicted by the model are in good agreement with model-independent experimental data over the entire ionic strength range from very dilute to ~4.5 m in alkaline solutions.

TABLE 5. Enthalpy changes for reactions involving zeolites derived in this study

Reactions	$\Delta_r H$, kJ/mol*
$Na_3HSiO_4 \cdot 2H_2O + 3H^+ = 3Na^+ + H_4SiO_4(aq) + 2H_2O(l)$	–58 ± 45 (2σ)
$NaAlSiO_4 \cdot 2.25H_2O$(cr, zeolite A) + $4H^+ = Na^+ + Al^{3+} + H_4SiO_4(aq) + 2.25H_2O(l)$	–152 ± 5 (2σ)
$NaAlSiO_4 \cdot 2.25H_2O$(am, zeolite A) + $4H^+ = Na^+ + Al^{3+} + H_4SiO_4(aq) + 2.25H_2O(l)$	–248 ± 3 (2σ)

* Uncertainties account for the errors from regressions only. The overall uncertainties could be higher than those provided here.

Model applications

In the following, the model developed above is applied to calculations of speciation of silica species as a function of pH at temperatures of 25 and 100 °C, and to retrieval of thermodynamic data from hydrothermal solubility data on zeolite A and amorphous precursor of zeolite A.

Speciation of silica species

In Figures 5a–5c, speciation of silica species as a function of pH at 25 °C at different total silica concentrations is displayed. At ΣSi = 0.01 m, monomer species are the dominant species (Fig. 5a). In the pH range from ~7 to ~9, the polymeric species $H_5Si_2O_7^-$ can account for up to 2% of the total dissolved silica (Fig. 5a). At ΣSi = 0.1 m, although monomer species are still the dominant species, contributions from polymeric species become significant (Fig. 5b). In the pH range from ~6 to ~10, $H_5Si_2O_7^-$ can account for up to ~20% of the total dissolved silica. In the pH range from ~9 to ~13, both $H_4Si_2O_7^{2-}$ and $H_5Si_3O_{10}^{3-}$ can account for up to ~5% of the total dissolved silica (Fig. 5b). At ΣSi = 1 m, contributions from polymeric species to the total dissolved silica become important (Fig. 5c). In the pH range up to 9, $H_5Si_2O_7^-$ can account for up to ~50% of the total dissolved

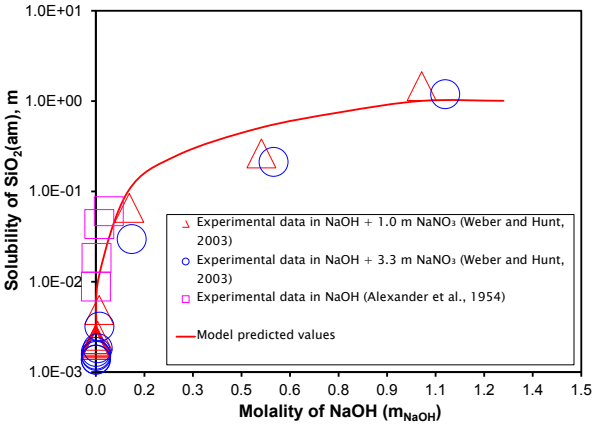

FIGURE 4. Comparison of model predicted solubilities of amorphous silica with experimental values, which are independent from the model development. The size of error bars is equal to or smaller than the symbol size. (Color online.)

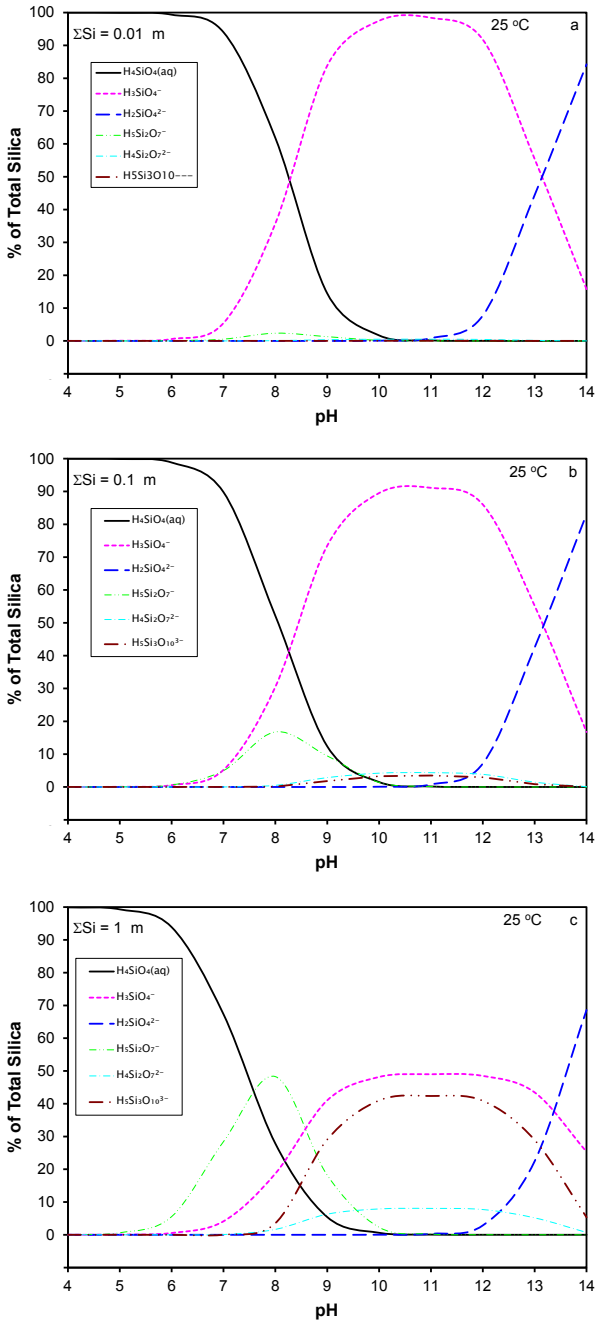

Figure 5. Speciation of silica at different total concentrations of silica as a function of pH at 25 °C. (**a**) Total silica concentration is 0.01 m; (**b**) total silica concentration is 0.1 m; and (**c**) total silica concentration is 1 m. Notice that in acidic pH range, the solution is supersaturated with amorphous silica. (Color online.)

silica. In the pH range from 8 to 14, $H_5Si_3O_{10}^{3-}$ can account for up to ~40% of the total dissolved silica, and $H_4Si_2O_7^{2-}$ can account for up to ~10% of the total dissolved silica. However, the trend indicates that $H_2SiO_4^{2-}$ will be the dominant species above pH 14 even at ΣSi = 1 m.

Similarly, speciation of silica at different total concentrations of silica as a function of pH at 100 °C is displayed in Figures 6a–6c. The polymeric silica species are important when ΣSi = 1 m (Fig. 6c). However, when pH higher than 11.5, the contributions from polymeric silica species diminish, and above pH 13, the contributions from polymeric silica species become insignificant (Fig. 6c).

It should be mentioned that under highly basic conditions where zeolites are formed as discussed below, $H_2SiO_4^{2-}$ is the dominant species.

Calculation of equilibrium constants of zeolites

Using the above thermodynamic model, the thermodynamic equilibrium constants of zeolites can be retrieved from solubility experiments at elevated temperatures. The main criterion of selection of solubility data is that equilibrium state must be attained. For precipitation and dissolution of zeolites at elevated temperatures, detailed kinetic studies have demonstrated that equilibrium state is rapidly attained. Addai-Mensah et al. (2004) performed detailed experiments from both undersaturation and supersaturation on zeolite A and amorphous precursor of zeolite A in NaOH solutions at 65 °C. Their experimental results demonstrate that the reversal was attained in about one minute (~50 s), indicating fast kinetics to reach equilibrium. Antonic et al. (1993) also indicated that the equilibrium was attained at about 20 min for dissolution of zeolite A at 80 °C. For experimental results in which the equilibrium state was not explicitly mentioned, steady-state concentrations after 100 min are treated as equilibrium concentrations. In this study, as sufficient data for zeolite A and amorphous precursor of zeolite A have been located, equilibrium constants for these two phases are computed. For zeolite X ($NaAlSi_{1.23}O_{4.46}\cdot 3.07H_2O$), Čižmek et al. (1991b) conducted solubility experiments on zeolite X in 2.06 m NaOH solution from 65 to 80 at 5 °C increment, and their data set has only one data point at each temperature. Roozeboom et al. (1983) had one single data point for solubility of zeolite X in ~1.02 m NaOH at 98 °C. Therefore, sufficient data have not been located for zeolite X. Consequently, no attempt has been made to compute equilibrium constants for zeolite X at this time.

Equilibrium constants are obtained according to the computer modeling. The computer modeling is performed by using EQ3/6 version 8.0a (Wolery et al. 2010; Xiong 2011). The essence of the modeling is to minimize the difference between experimental and model predicted values, as detailed in the previous publication (Nemer et al. 2011). The retrieval of the equilibrium constant for amorphous precursor of zeolite A at 30 °C can be served as an example. First, solubility data from Ejaz and Graham (1999) and Addai-Mensah et al. (2004) were used to generate EQ3NR input files. Second, an initial guess for the log *K* was made. Third, by changing the log *K* into different values, a series of sums of squares of residuals between experimental solubilities and predicted solubilities were obtained. The final log *K* corresponds to the minimized sum of squares of residuals.

Calculation of equilibrium constants of zeolite A

Several researchers have investigated solubilities of zeolite A in NaOH solutions at elevated temperatures. The sources of solubility data used for obtaining equilibrium constants in this

study and their respective experimental conditions are listed in Table 1. Based on those experimental data, the equilibrium constants for the following reaction using Al^{3+} and H_4SiO_4(aq) as basis species of aluminum and silica, respectively,

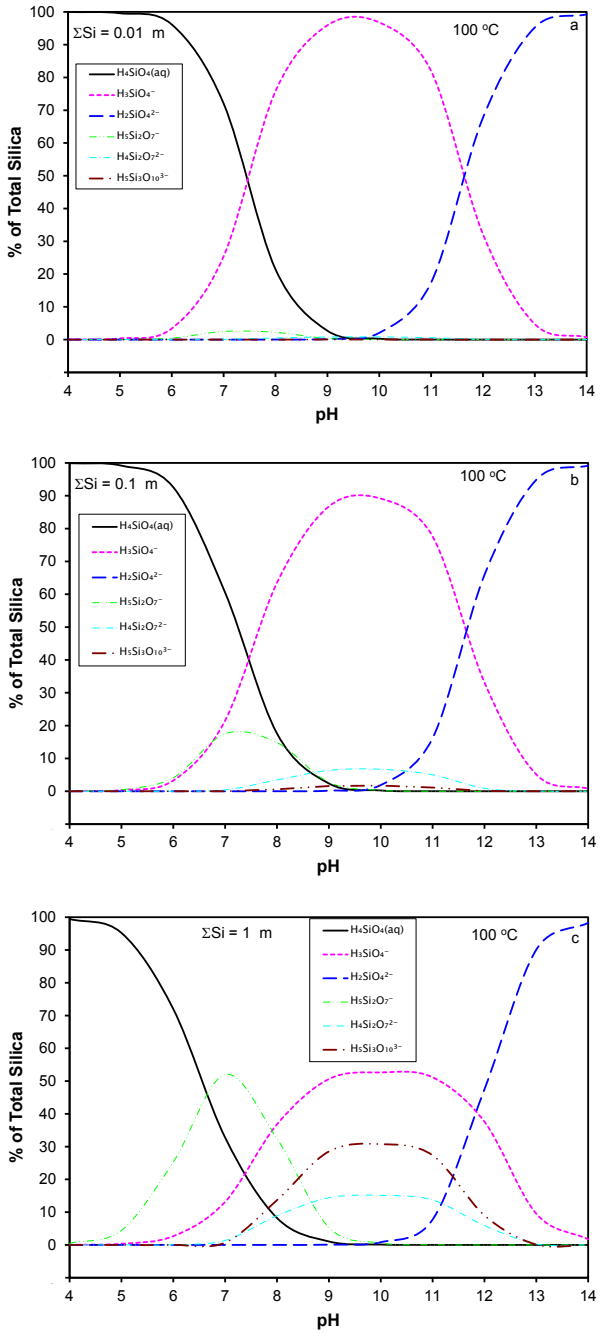

Figure 6. Speciation of silica at different total concentrations of silica as a function of pH at 100 °C. (**a**) Total silica concentration is 0.01 m; (**b**) total silica concentration is 0.1 m; and (**c**) total silica concentration is 1 m. Notice that in acidic pH range, the solution is supersaturated with amorphous silica/quartz. (Color online.)

$$NaAlSiO_4{\cdot}2.25H_2O(cr) + 4H^+ = Na^+ + Al^{3+} + H_4SiO_4(aq) + 2.25H_2O(l) \quad (21)$$

are obtained (Table 3). In computation of equilibrium constants, all concentrations on molar scale are converted to molal scale according to the following equation based on densities of supporting solutions used in experiments at respective temperatures, which are calculated from density equations of Sőhnel and Novotný (1985),

$$m_i = \frac{1000 \times M_i}{1000\rho - \sum_i^j M_i E_i} \quad (22)$$

where m_i is concentration of i species on molality scale, ρ density of solution, M_i is concentration of i species on molarity scale, and E_i the molecular weight of i species.

In Figure 7, predicted solubilities of zeolite A at temperatures of 30, 65, 70, 80, 90, and 100 °C, are compared with experimental data at the respective temperatures. At 30 °C, there is a scatter in experimental data from various researchers with a difference of one order of magnitude, and the model seems to fit experimental data within a factor of ~5 except for that it underpredicts at $I \approx$ 6 m by a factor of ~7 (Fig. 7a). At 50 °C, the values produced by the model agree with experimental values within a factor of ~1.3 (Fig. 7a). At 65 °C, the model reproduces experimental data within a factor of ~2 (Fig. 7a). At 70 °C, the values predicted by the model agree with experimental values within a factor of ~1.4 (Fig. 7b). At 80 °C, the model reproduces solubilities in the ionic strength range from ~3 to ~5 m within a factor of ~3.5 in comparison with the experimental data (Fig. 7b), whereas solubilities predicted by the model agree with experimental solubilities within a factor of ~1.1 in the ionic strength range from ~0.5 to ~2 m. At 90 °C, solubilities calculated by the model generally agree with experimental values within a factor of ~2 (Fig. 7c). At 100 °C, solubilities computed by the model are in agreement with experimental values within a factor of ~1.2 (Fig. 7c). In all above descriptions, the Al-Si complex, $Al(OH)_3HSiO_4^{3-}$, was not included in calculations.

At 30 °C, the inclusion of $Al(OH)_3HSiO_4^{3-}$ yields a log K of 9.96 ± 0.30 for reaction 21, in comparison with a value of 10.23 ± 0.31 for the log K produced by the model without the above Al-Si complex. These two values are statistically indistinguishable. However, as indicated by Figure 7a, the introduction of the above Al-Si complex improves the fitting at 30 °C; the model reproduces the solubility at $I \approx$ 6 m within a factor of ~2 in comparison with the experimental data point. Notice that as described before, the model without $Al(OH)_3HSiO_4^{3-}$ reproduces the solubility at that ionic strength within a factor of ~7.

On the other hand, at 50 °C, the model with the Al-Si complex produces a log K of 7.41 ± 0.40 for reaction 21, whereas the model without the Al-Si complex results in a log K of 7.95 ± 0.30. Figure 7a shows that the model without the Al-Si complex performs better. The reason for the poor performance of the model with Al-Si complex is not clear. One possibility may be that the existence of the Al-Si complex at 50 °C is uncertain, as Gout et al. (2000) only mentioned its presence at 20 °C. The model with the Al-Si complex at 30 °C is close to 20 °C, and

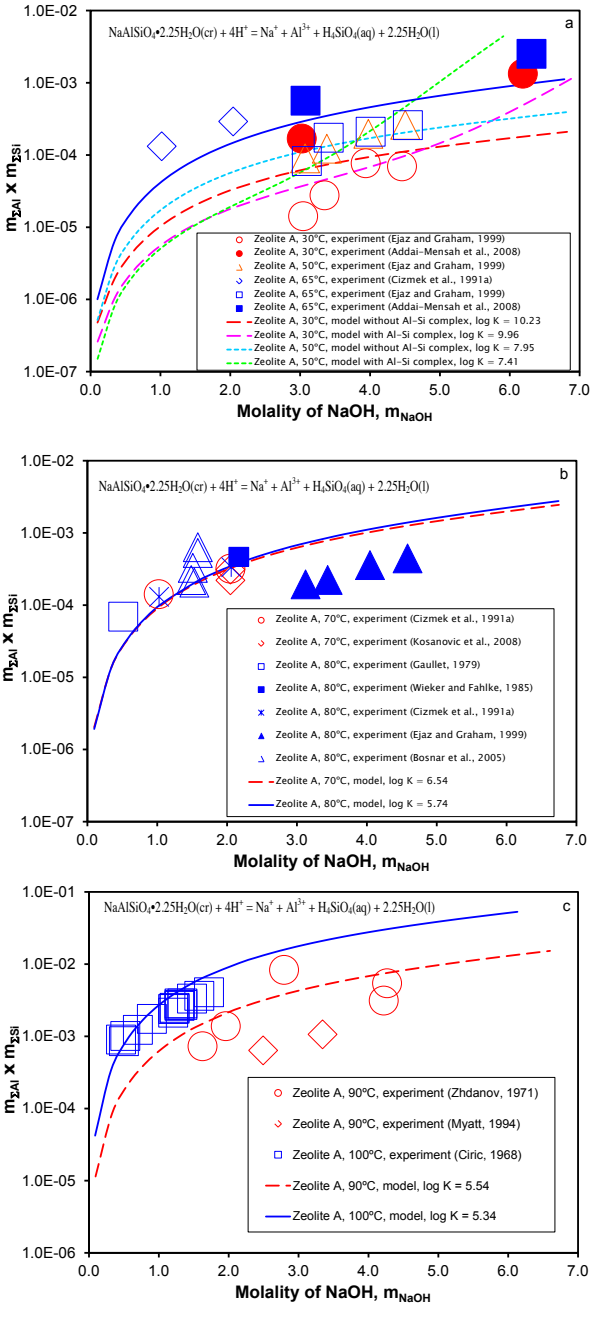

FIGURE 7. Comparison of model predicted solubilities of zeolite A with experimental values: (**a**) at 30, 50, and 65 °C; (**b**) at 70 and 80 °C; and (**c**) at 90 and 100 °C. The size of error bars is equal to or smaller than the symbol size. (Color online.)

the presence of the Al-Si complex at 30 °C is of high certainty, if there is such a complex, explaining the better performance of the model with the Al-Si complex at 30 °C. Another possibility is that the Pitzer parameters for Na^+-$Al(OH)_3HSiO_4^{3-}$ might be problematic. This seems unlikely, as the same set of parameters is also used at 30 °C, which results in a desirable performance. However, the final resolution of this issue requires independent evaluation of the Pitzer parameters and to see if they can improve the model with the Al-Si complex.

Judging from the performance of the models with and without the Al-Si complex at 30 and 50 °C, it can be concluded that the model without the Al-Si complex is adequate at temperatures equal to or higher than 50 °C. Therefore, no further testing was performed at higher temperatures. Anyhow, the testing at 30 °C seems to provide independent support for the existence of $Al(OH)_3HSiO_4^{3-}$ around 20 °C.

Based on the linear regression of temperature dependence of equilibrium constants, $\Delta_r H$ for reaction 21 is derived as –152 ± 5 kJ/mol (Table 5). According to Figure 8, the log K at 25 °C is extrapolated as 10.24 ± 0.31. Using the above thermodynamic properties for reaction 21, the thermodynamic properties of zeolite A at 25 °C and 1 bar are derived (Table 6). In derivation of these thermodynamic properties, the auxiliary thermodynamic data for Na^+ and Al^{3+} are from the DATA0.PIT database. The auxiliary thermodynamic data for H_4SiO_4(aq), which are not present in the DATA0.PIT database, are from the NBS Thermodynamic Table (Wagman et al. 1982). The latter database is in principle consistent with the DATA0.PIT database. However, as the thermodynamic properties obtained in this study are log K values and $\Delta_r H$, Gibbs free energies of formation, enthalpies of formation, and standard entropies can be re-derived to be consistent with other database(s) of interest, if needed.

Calculation of equilibrium constants of amorphous precursor of zeolite A

In the synthesis of zeolite A, its amorphous precursor is usually formed first. Therefore, it is also important to know the thermodynamic properties of the amorphous precursor of zeolite A to optimize synthesis. Similar to reaction 21, the dissolution reaction of the amorphous precursor of zeolite A is:

$$NaAlSiO_4 \cdot 2.25H_2O(am) + 4H^+ = Na^+ + Al^{3+} + H_4SiO_4(aq) + 2.25H_2O. \quad (23)$$

Ejaz and Graham (1999) conducted systematic solubility studies on the amorphous precursor of zeolite A in NaOH solutions from 3.0 to 4.5 m at temperatures of 30, 50, 65, and

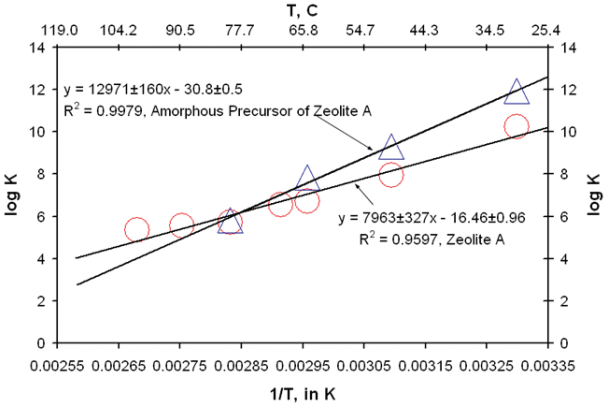

FIGURE 8. A plot showing equilibrium constants of zeolite A and amorphous precursor of zeolite A as a function of reciprocal temperatures in Kevin. The size of error bars is equal to or smaller than the symbol size. (Color online.)

TABLE 6. Thermodynamic properties of zeolite A and the amorphous form of zeolite A at 25 °C and 1 bar derived in this study*

Properties	Values (± 2σ)	Remarks
$\Delta_f H°$, Zeolite A, $NaAlSiO_4$•2.25H_2O(cr)	−2738 ± 5 kJ/mol	Based on $\Delta_r H$ derived from temperature dependence of equilibrium constant.
$\Delta_f G°$, Zeolite A, $NaAlSiO_4$•2.25H_2O(cr)	−2541 ± 2 kJ/mol	Based on $\Delta_r G$ derived from log *K* extrapolated to 25 °C.
S°, Zeolite A, $NaAlSiO_4$•2.25H_2O(cr)	373 ± 10 J/(K·mol)	Based on $\Delta_r S$ calculated from the Gibbs-Helmholtz equation.
$\Delta_f H°$, Amorphous precursor of zeolite A, $NaAlSiO_4$•2.25H_2O(am)	−2642 ± 3 kJ/mol	Based on $\Delta_r H$ derived from temperature dependence of equilibrium constant.
$\Delta_f G°$, Amorphous precursor of zeolite A, $NaAlSiO_4$•2.25H_2O(am)	−2527 ± 2 kJ/mol	Based on $\Delta_r G$ derived from log *K* extrapolated to 25 °C.
S°, Amorphous precursor of zeolite A, $NaAlSiO_4$•2.25H_2O(am)	648 ± 10 J/(K·mol)	Based on $\Delta_r S$ calculated from the Gibbs-Helmholtz equation.

* All properties refer to formation from elements.

80 °C (Table 1). In addition, Addai-Mensal et al. (2004) also conducted solubility experiments on amorphous precursor of zeolite A in 3.0 and 6.3 m NaOH solutions at 30 and 65 °C (Table 1). Therefore, based on solubility data from both Ejaz and Graham (1999) and Addai-Mensal et al. (2004), the equilibrium constants for the amorphous precursor of zeolite A are calculated (Table 4).

In Figure 9, predicted solubilities of amorphous precursor of zeolite A are compared with experimental data. At 30 and 50 °C, the solubility curves for these two temperatures are very close, and the solubilities predicted by the model match experimental values within a factor of ~1.6 (Fig. 9a). At 65 °C, the solubilities predicted by the model are in agreement with experimental values within a factor of ~2.5 for the majority of the data points, and within a factor of ~4.5 for the data point at $I \approx 6$ m (Fig. 9b). At 80 °C, the model matches the experimental solubilities in high ionic strength range within a factor of ~2, but within a factor of ~5 to ~10 at a low ionic strength (~0.2 m) (Fig. 9b).

According to the linear regression of temperature dependence of equilibrium constants (Fig. 8), $\Delta_r H$ for reaction 23 is obtained as –248 ± 3 kJ/mol (Table 5). Based on Figure 8, the log *K* for reaction 23 at 25 °C is extrapolated as 12.68 ± 0.35. In accordance with the above thermodynamic properties for reaction 23, the thermodynamic properties of amorphous precursor of zeolite A at 25 °C and 1 bar are derived (Table 6).

Validation of calculations and discussions

The enthalpy of formation for zeolite A derived from solubility studies as a function of temperature in this study is compared with the value from calorimetric measurements. The enthalpy of formation from elements for zeolite A obtained in this study, –2738 ± 5 kJ/mol, is in excellent agreement with the value obtained by calorimetric measurements (–2731.3 ± 1.8 kJ/mol) (Turner et al. 2008), and compares favorably with the value obtained by theoretical calculations (–2739 kJ/mol) (Mathieu and Viellard 2010). In these two studies, zeolite A is formulated as $Na_{0.5067}Al_{0.501}Si_{0.4974}O_{1.99965}$·1.0906$H_2O$. For comparison purpose, their values are scaled relative to four oxygen atoms for the stoichiometry of zeolite A adopted in this study, i.e., $NaAlSiO_4$·2.25H_2O. This favorable comparison also validates the model developed in this study.

The Gibbs free energy of formation for zeolite A at 25 °C obtained in this study can also be compared with that of Caullet et al. (1980). Caullet et al. (1980) determined the log *K* for zeolite A with a formula of $NaAlSi_{1.06}O_{4.12}$·2.4H_2O for the following reaction from solubility experiments in 0.02, 0.1, and 0.5 m NaOH solutions at 25 °C,

$$NaAlSi_{1.06}O_{4.12}\cdot 2.4H_2O + 1.72\ H_2O(l) = Al(OH)_4^- + 1.06\ H_4SiO_4(aq) + Na^+. \quad (24)$$

The average thermodynamic equilibrium constant, log *K* at 25 °C, for reaction 24 obtained by Caullet et al. (1980) is –11.20 ± 0.16. Based on the log *K* value for reaction 24, the Gibbs free energy change for reaction 24 is calculated as 63.9 ± 0.9 kJ/mol. According to the auxiliary thermodynamic data for species in reaction 24 from the NBS Thermodynamic Table, the Gibbs free energy of formation, $\Delta_f G$, for $NaAlSi_{1.06}O_{4.12}$·2.4H_2O, is derived as –2619 ± 2 kJ/mol. When it is scaled to four oxygen atoms for the stoichiometry of zeolite A adopted in this study, in the same procedure applied in the above validation of calculation of enthalpy of formation for zeolite A, the Gibbs free energy

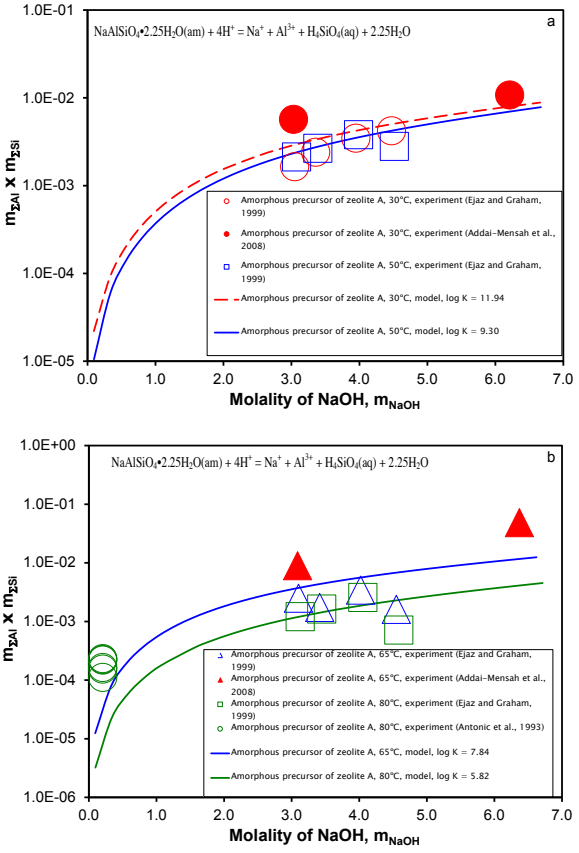

FIGURE 9. Comparison of model predicted solubilities of amorphous precursor of zeolite A with experimental values: (**a**) at 30 and 50 °C; and (**b**) at 65 and 80 °C. The size of error bars is equal to or smaller than the symbol size. (Color online.)

of formation becomes –2543 ± 2 kJ/mol for the formula of $Na_{0.97}Al_{0.97}Si_{1.03}O_4{\cdot}2.33H_2O$. This value is in good agreement with the value of –2541 ± 2 kJ/mol obtained in this study. The corresponding log *K* at 25 °C for the following reaction,

$$Na_{0.97}Al_{0.97}Si_{1.03}O_4{\cdot}2.33H_2O(cr) + 3.88H^+ = 0.97Na^+ + 0.97Al^{3+} + 1.03H_4SiO_4(aq) + 2.21H_2O(l) \quad (25)$$

would be 11.33 ± 0.20. Qiu et al. (2000) measured the entropy of dehydrated zeolite A with a formula of $Na_{96}Al_{96}Si_{96}O_{394}$ as 13 030 J/(K·mol) at 25 °C. When the above formula is scaled to four oxygen atom, the corresponding entropy becomes 135.73 J/(K·mol) for dehydrated zeolite A with a formula of $NaAlSiO_4$. Viellard (2010) uses a value of 52.0 J/(K·mol) for the entropy of zeolitic water for predictions of entropies of zeolites. Accordingly, using the above values from Qiu et al. (2000) and Viellard (2010), the entropy for zeolite A with a formula of $NaAlSiO_4{\cdot}2.25H_2O$ would be expected to be 253 J/(K·mol). This value would differ by about 100 J/(K·mol) from the entropy obtained in this study, which was consistently derived from $\Delta_r H$ and $\Delta_r G$ from equilibrium observations. As the enthalpy of formation for zeolite A derived in this study is consistent with the value obtained by the calorimetric method as mentioned above, we might use $\Delta_f H$ = –2738 kJ/mol and $S°$ = 253 J/(K·mol) for zeolite A to calculate the log *K* at 25 °C for reaction 21. That would result in a value for the log *K* at 25 °C for reaction 21 to be 16.50. This value is severely discordant with the log *K* (10.23 ± 0.31) for reaction 21 obtained in this study, and the similar log *K* (11.33 ± 0.20) for reaction 25 obtained by Caullet et al. (1980), both at 25 °C, and it would predict solubilities of zeolite A by at least five orders of magnitude higher than the observed solubilities. Therefore, it seems that further studies on entropies of both zeolite A and dehydrated zeolite A by calorimetric measurements are required, as the existing value does not agree with equilibrium observations.

Concluding remarks

In this study, a thermodynamic model for silica and aluminum is developed, valid to high ionic strength at elevated temperatures up to 100 °C. This model is useful for understanding the geochemical behaviors of Si and Al in concentrated hydrothermal solutions, and for guiding hydrothermal synthesis of zeolites. This model enable us to calculate equilibrium constants of sodium silicates, zeolite A, and amorphous precursor of zeolite A, from hydrothermal solubility experiments. In the near future, equilibrium constants for other zeolite species such as sodalite and cancrinite will be evaluated from hydrothermal experiments. Because of the discordance of one single existing entropy for dehydrated zeolite from calorimetric measurements with equilibrium observations, it is suggested that further calorimetric studies on both zeolite A and dehydrated zeolite A are needed to resolve such a discordance.

Acknowledgments

Sandia National Laboratories is a multi-program laboratory managed and operated by Sandia Corporation, a wholly owned subsidiary of Lockheed Martin Corporation, for the U.S. Department of Energy's National Nuclear Security Administration under contract DE-AC04-94AL85000. The author thanks Bill Bourcier, Philip Neuhoff, and an anonymous reviewer for their detailed and insightful reviews, which have significantly improved the quality of the presentation. The journal editors, Jenny Thomson, Keith Putirka, and the associate editor, Rick Wilkin, are thanked for their editorial efforts.

References cited

Addai-Mensah, J., Li, J., Rosencrance, S., and Wilmarth, W. (2004) Solubility of amorphous sodium aluminosilicate and zeolite A crystals in caustic and nitrate/nitrite-rich caustic aluminate liquors. Journal of Chemical and Engineering Data, 49, 1682–1687.

Alexander, G.B., Heston, W.M., and Iler, R.K. (1954) The solubility of amorphous silica in water. Journal of American Chemical Society, 58, 453–455.

Antonić, T., Čižmek, A., Kosanović, C., and Subotić, B. (1993) Dissolution of amorphous aluminosilicate zeolite precursors in alkaline solutions. Journal of Chemical Society Faraday Transactions, 89, 1817–1822.

Azaroual, M., Fouillac, C., and Matray, J.M. (1997) Solubility of silica polymorphs in electrolyte solutions, I. Activity coefficient of aqueous silica from 25 °C to 250 °C, Pitzer's parameterization. Chemical Geology, 140, 155–165.

Baes, C.F. and Mesmer, R.E. (1976) The Hydrolysis of Cations. Wiley, New York.

Baker, C.L., Jue, L.R., and Wills, J.H. (1950) The system Na_2O–SiO_2–H_2O at 50, 70 and 90 °C. Journal of Physical Chemistry, 72, 5369–5382.

Bosnar, S., Bronić, J., Krznarić, I., and Subotić, B. (2005) Influence of the concentrations of aluminium and silicon in the liquid phase on the growth kinetics of zeolite A and X microcrystals. Croatica Chemica Acta, 78, 1–8.

Busey, R.H. and Mesmer, R.E. (1977) Ionization of silicic acid and polysilicate formation in aqueous chloride solutions to 300 °C. Inorganic Chemistry, 16, 2444–2453.

Castet, S., Dandurand, J., Schott, J., and Gout, R. (1993) Boehmite solubility and aqueous aluminum speciation in hydrothermal solutions (90–350 °C): Experimental study and modeling. Geochimica et Cosmochimica Acta, 57, 4869–4884.

Caullet, P., Guth, J.-L., and Wey, R. (1980) Solubilité et grandeurs thermodynamiques de dissolution des zéolites 4A et 13X dans des solutions aqueuses basiques. Bulletin de Minéralogie, 103, 330–335.

Chorover, J., Choi, S., Amistadi, M.K., Karthikeyan, K.G., Crosson, G., and Mueller, K.T. (2003) Linking cesium and strontium uptake to kaolinite weathering in simulated tank waste leachate. Environmental Science and Technology, 37, 2200–2208.

Ciric, J. (1968) Kinetics of zeolite A crystallization. Journal of Colloid and Interface Science, 28, 315–324.

Čižmek, A., Komunjer, L., Subotić, B., Široki, M., and Rončević, S. (1991a) Kinetics of zeolite dissolution: Part 1. Dissolution of zeolite A in hot sodium hydroxide. Zeolites, 11, 258–264.

——— (1991b) Kinetics of zeolite dissolution: Part 2. Dissolution of zeolite X in hot sodium hydroxide. Zeolites, 11, 810–815.

——— (1992) Kinetics of zeolite dissolution: Part 3. Dissolution of synthetic mordenite in hot sodium hydroxide. Zeolites, 12, 190–196.

Ejaz, T. and Graham, A.G.J. (1999) Solubility of zeolite A and its amorphous precursor under synthesis conditions. Journal of Chemical and Engineering Data, 44, 574–576.

Felmy, A.R., Cho, H., Rustad, J.R., and Mason, M.J. (2001) An aqueous thermodynamic model for polymerized silica species to high ionic strength. Journal of Solution Chemistry, 30, 509–525.

Flemıng, B.A. and Crerar, D.A. (1982) Silicic acid ionization and calculation of silica solubility at elevated temperature and pH. Application to geothermal fluid processing and re-injection. Geothermics, 11, 15–29.

Gout, R., Pokrovski, G.S., Schott, J., and Zwick, A. (2000) Raman spectroscopic study of aluminum silicate complexes at 20°C in basic solutions. Journal of Solution Chemistry, 29, 1173–1186.

Grenthe, I., Fuger, J., Konings, R.J.M., Lemire, R.J., Muller, A.B., Nguyen-Trung, C., and Wanner, H. (1992) Chemical thermodynamics of uranium. In H. Wanner and I. Forest, Eds., Nuclear Energy Agency, Organization for Economic Co-operation, Development, vol. 1, Chemical Thermodynamics, 715 p. Elsevier, Amsterdam.

Gu, Y., Gammons, C., and Bloom, M.S. (1994) A one-term extrapolation method for estimating equilibrium constants of aqueous reactions at elevated temperatures. Geochimica et Cosmochimica Acta, 58, 3545–3560.

Helgeson, H.C. and Kirkham, D.H. (1974) Theoretical prediction of the thermodynamic behavior of aqueous electrolytes at high pressures and temperatures. II. Debye–Hückel parameters for activity coefficients and relative partial molal properties. American Journal of Sciences, 274, 1199–1261.

Hershey, J.P. and Millero, F.J. (1986) The dependence of the acidity constants of silicis acid on NaCl concentration using Pitzer's equation. Marine Chemistry, 18, 101–105.

Hunt, J.D., Kavner, A., Schauble, E.A., Snyder, D., and Manning, C.E. (2011) Polymerization of aqueous silica in H_2O–K_2O solutions at 25–200 °C and 1 bar to 20 kbar. Chemical Geology, 283, 161–170.

Johnson, J.W., Olkers, E.H., Helgeson, H.C. (1992) SUPCRT92: A software package for calculating the standard molal thermodynamic properties of minerals, gases, aqueous species, and reactions from 1 to 5000 bar and 0 to 1000°C.

Computers and Geosciences, 18, 899–947.
Kosanović, C., Subotić, B., Kaučič, V., and Škreblin, M. (2000) Dissolution of the zeolites NaA, potassum exchanged zeolite (KA) and the amorphous and crystalline phases obtained by thermal treatment of zeolite KA in hot alkaline solution. Physical Chemistry and Chemical Physics, 2, 3447–3451.
Mashal, K., Harsh, J.B., Flury, M., and Felmy, A.R. (2004) Colloid formation in Hanford sediments reacted with simulated tank waste. Environmental Science and Technology, 38, 5750–5756.
Mathieu, R. and Vieilard, P. (2010) A predictive model for the enthalpy formation of zeolites. Microporous and Mesoporous Materials, 132, 335–351.
Moolenaar, R.J., Evans, J.C., and McKeever, L.D. (1970) The structure of the aluminate ion in solutions at high pH. Journal of Physical Chemistry, 74, 3629–3636.
Myatt, G.J., Budd, P.M., Price, C., Hollway, F., and Carr, S.E. (1994) The influence of surfactants and water-soluble polymers on the crystallization of zeolite NaA. Zeolites, 14, 190–197.
Nemer, M., Xiong, Y.-L., Ismail, A.E., and Jang, J.-H. (2011) Solubility of $Fe_2(OH)_3Cl$ (pure-iron end-member of hibbingite) in NaCl and Na_2SO_4 brines. Chemical Geology, 280, 26–32.
Pitzer, K.S. (1991) Ion interaction approach: theory and data correlation. In K.S. Pitzer, Ed., Activity Coefficients in Electrolyte Solutions, 2nd ed., p. 75–153. CRC Press, Boca Raton, Florida.
Plyasunov, A., Fanghanel, T., and Grenthe, I. (1998) Estimation of the Pitzer equation parameters for aqueous complexes. A case study for uranium at 298.15 K and 1 atm. Acta Chemica Scandinavica, 52, 250–260.
Pokrovski, G.S., Schott, J., Salvi, G., Gout, R., and, Kubicki, J.D. (1998) Structure and stability of aluminium-silica complexes in neutral to basic solutions. Experimental study and molecular orbital calculations. Mineralogical Magazine, 62A, 1194–1195.
Qiu, L.-Y., Murashov, V., and White, M.A. (2000) Zeolite 4A: heat capacity and thermodynamic properties. Solid State Science, 2, 841–846.
Roozeboom, F., Robson, H.E., and Chan, S. (1983) Laser Raman study on the crystallization of zeolites A, X, and Y. Zeolites, 3, 321–328.
Salvi, S., Pokrovski, G.B., and Schott, J. (1998) Experimental investigation of aluminum-silica aqueous complexing at 300°C. Chemical Geology, 151, 51–67.
Šefčik, J. and McCormick, A.V. (1997a) What is the solubility of zeolite A. Microporous Materials, 10, 173–179.
——— (1997b) Thermochemistry of aqueous silicate solution precursors to ceramics. AIChE Journal, 43, 2773–2784.
Serne, R.J., Clayton, R.E., Kutnyakov, I.V., Last, G.V., LeGore, V.L., Wilson, T.C., Schaef, H.T., O'Hara, M.J., Wagnon, K.B., Lanigan, D.C., and others. (2002) Characterization of Vadose Zone Sediment: Borehole 41-09-39 in the S-SX Waste Management Area. Pacific Northwest National Laboratory, U.S. Department of Energy, PNNL-13757-3, Richland, Washington.
Seward, T.M. (1974) Determination of the first ionization constant of silicic acid from quartz solubility in borate buffer solutions to 350 °C. Geochimica et Cosmochimica Acta, 38, 1651–1664.
Sheppard, G.P., Hriljac, J.A., Maddrell, E.R., Hyatt, N. (2006) Silver zeolites: Iodide occlusion and conversion to sodalite-a potential ^{129}I waste form? Materials Research Society Symposium Proceeding, vol. 932, 8 pp.
Sőhnel, O. and Novotný, P. (1985) Densities of Aqueous Solutions of Inorganic Substances, 335 p. Elsevier, New York.
Sprauer, J.W. and Pearce, D.W. (1940) Equilibrium in the systems Na_2O–SiO_2–H_2O and Na_2O–Al_2O_3–H_2O at 25 °C. Journal of American Chemical Society, 44, 909–916.
Tagirov, B., and Schott, J. (2001) Aluminum speciation in crustal fluids revisited. Geochimica et Cosmochimica Acta, 65, 3965–3992.
Turner, S., Sieber, J.R., Vetter, T.W., Zeisler, R., Marlow, A.F., Moreno-Ramirez, M.G., Davis, M.E., Kennedy, G.J., Borghard, W.G., Yang, S., and others. (2008) Characterization of chemical properties, unit cell parameters and particle size distribution of three zeolite reference materials: RM 8850 – zeolite Y, RM 8851 – zeolite A and RM 8852 – ammonium ZSM-5 zeolite. Microporous and Mesoporous Materials, 107, 252–267.
Viellard, P. (2010) A predictive model for the entropies and heat capacities of zeolites. European Journal of Mineralogy, 22, 823–836.
Wagman, D.D., Evans, W.H., Parker, V.B., Schumm, R.H., Halow, I., Bailey, S., Churney, K., and Nuttall, R.L. (1982) The NBS tables of chemical thermodynamic properties: Selected values for inorganic and C_1 and C_2 organic substances in SI units. Journal of Physical and Chemical Reference Data, vol. 11, Supplement No. 2, 392 pp.
Weber, C. and Hunt, R.D. (2003) Modeling alkaline silicate solutions at 25 °C. Industrial Engineering and Chemical Research, 42, 6970–6976.
Wesolowski, D.J. (1992) Aluminum speciation and equilibrium in aqueous solution: I. The solubility of gibbsite in the system Na-K-Cl-OH-$Al(OH)_4$ from 0 °C to 100 °C. Geochimica et Cosmochimica Acta, 56, 1065–1091.
Wieker, W. and Fahlke, B. (1985) On the reaction mechanism of the formation of molecular sieve and related compounds. In Drzaj, B., Hocevar, S., Pejovnik, S., Eds., Zeolites, p. 161–181. Elsevier, Amsterdam.
Wolery, T.J. (1992) EQ3/6, A Software Package for Geochemical Modeling of Aqueous Systems: UCRL-MA-110662 PT I. Lawrence Livermore National Laboratory, Livermore, California.
Wolery, T.W., Xiong, Y.-L., and Long, J. (2010) Verification and Validation Plan/Validation Document for EQ3/6 Version 8.0a for Actinide Chemistry, Document Version 8.10. Sandia National Laboratories, Carlsbad, New Mexico, ERMS 550239.
Xiong, Y.-L. (2003) Predicted equilibrium constants for solid and aqueous selenium species to 300 °C: Applications to selenium-rich mineral deposits. Ore Geology Reviews, 23, 259–276.
——— (2007) Hydrothermal thallium mineralization up to 300 °C: A thermodynamic approach. Ore Geology Reviews, 32, 291–313.
——— (2011) WIPP Verification and Validation Plan/Validation Document for EQ3/6 Version 8.0a for Actinide Chemistry, Revision 1, Document Version 8.20. Supersedes ERMS 550239. Sandia National Laboratories, Carlsbad, New Mexico, ERMS 555358.
Yokoyama, T., Kinoshita, S., Wakita, H., and Tarutani, T. (1988) ^{27}Al NMR study on the Interaction between aluminate and silicate ions in alkaline solution. Bulletin of the Chemical Society of Japan, 61, 1002–1004.
Zhao, H., Deng, Y., Harsh, J.B., Flury, M., and Boyle, J. (2004) Alteration of kaolinite to cancrinite and sodalite by simulated Hanford Tank Wastes and its impact on cesium retention. Clays Clay Mineralogy, 52, 1–13.
Zhdanov, S.P. (1971) Some problems of zeolite crystallization. In E.M. Flanigen and L.B. Sand, Eds., Molecular Sieve Zeolites-I, p. 20–43. American Chemical Society, Washington, D.C.
Zhou, J., Chen, Q.-Y., Li, J., Yin, Z.-L., Zhou, X., and Zhang, P.-M. (2003) Isopiestic measurement of the osmotic and activity coefficients for the NaOH–$NaAl(OH)_4$–H_2O system at 313.2 K. Geochimica et Cosmochimica Acta, 67, 3459–3472.

Manuscript received December 26, 2011
Manuscript accepted August 23, 2012
Manuscript handled by Richard Wilkin